Desalination and Water Treatment
www.deswater.com
doi: 10.5004/dwt.2020.25811

193 (2020) 177–188
July

Preparation and characterization of a high flux nanofiltration polyamide hollow fiber TFC membrane for drinking water production

Wan Su[a], Yufeng Zhang[a,b,*], Wenjuan Zhang[a,*], Shuting Xie[a], Xiaobo Sun[b], Jianqiang Meng[b]

[a]*Tianjin Key Laboratory of Aquatic Science and Technology, School of Environmental and Municipal Engineering, Tianjin Chengjian University, Tianjin 300384, China, emails: zyf9182@tjpu.edu.cn (Y. Zhang), wenjuanvivian@126.com (W. Zhang), 2587103926@qq.com (W. Su), 806741515@qq.com (S. Xie)*
[b]*State Key Laboratory of Separation Membranes and Membrane Processes, Tianjin Polytechnic University, Tianjin 300387, China, emails: sunxiaobo1016@163.com (X. Sun), jianqiang.meng@hotmail.com (J. Meng)*

Received 18 July 2019; Accepted 2 March 2020

ABSTRACT

In this study, a nanofiltration (NF) polyamide hollow fiber thin film composite membrane with a low rejection and a high flux was prepared in consideration of the "trade-off" relation between salt rejection and permeate flux of the membrane. The membrane was able to retain the beneficial minerals in tap water while keeping the body healthy. The membrane prepared had a thinner active skin layer (<100 nm) than those of commercial membranes. A permeability of 30.07 L/m²/h and a rejection rate of 79.68% for 1,000 mg/L $MgSO_4$ at 0.2 MPa were obtained. In addiiton, Fe^{3+}, Cu^{2+}, and Pb^{2+} were used to evaluate the heavy metal removal performance of the NF membrane. It was found that as the concentration of heavy metal ions increased to three times of the Standards for Drinking Water Quality (SDWQ) (GB5749-2006), and the rejections to all heavy metal ions were more than 76%. In addition, the NF membrane had a good long-term rejection stability for the heavy metal ions over a 12-month dynamic filtration experiment. The results showed that the newly prepared NF membrane has a good application prospect for domestic water purification.

Keywords: Nanofiltration membrane; Hollow fiber; Interfacial polymerization; Beneficial minerals; Heavy metal ions

1. Introduction

With the improvement of living standards, people are increasingly demanding for quality drinking water. It is believed that for drinking water it is not the purer the better, and people still need to drink water containing minerals and no harmful substances [1]. Healthy water should be safe and harmless to the human body, and at the same time, it must also be nutritious and retain the trace elements beneficial to the human body [2].

The emerging membrane separation and purification technology in the water treatment industry has brought processes for producing safe and healthy drinking water [3]. Various membrane treatment technologies, including ultrafiltration (UF), nanofiltration (NF), and reverse osmosis (RO), are increasingly used for treatment of drinking water [4,5].

UF membranes typically have a pore diameter of 0.002 to 0.1 μm and an operating pressure of 0.04 to 0.4 MPa. UF mainly targets at removal of macromolecular substances, suspended solids, colloids, and bacteria in water, whereas inorganic salts are not removed by UF [6]. RO membranes have a pore size of less than 0.001 μm and are capable of removing all substances in the water, including some minerals beneficial to the human body. The pH value of RO water is normally 5.8–6, which is below the pH of 6.5–8.5

* Corresponding authors.

per Standards for Drinking Water Quality (SDWQ) (GB5749-2006). In addition, the operating pressure for RO is between 1 and 10 MPa, and the energy consumption is quite large [7]. Therefore, there is a need for a membrane separation technique that has a better filtration effect than UF, and has a lower solute rejection and greater permeate flux than RO.

NF membrane is a membrane process between UF and RO. It has a higher removal rate for natural organic matter, trace organic compounds, and hardness ions (Ca^{2+}, Mg^{2+}, etc.) [8], and can achieve a higher water flux at a lower pressure. NF membranes have a pore size of less than 2 nm and a molecular weight cut-off (MWCO) of between 150 and 2,000 Daltons [9]. NF has been applied widely in the beverage production [10], treatment of polluted water [11] and wastewater [12], dye separation [13,14], food, and dairy processing [15], but rarely in drinking water treatment [1]. NF membrane mainly has two significant separation mechanism: the sieving effect and the Donnan effect [16]. The sieving effect is mainly used for separation of substances with different molecular weights. The Donnan effect refers to the electrostatic effect between the charges carried on the membrane and the ions distributed in the solution. NF membrane is capable of making discriminatory rejection between multivalent and monovalent salt ions owing to the charges on the membrane surface [17]. It can remove heavy metals and other substances that cannot be purified by UF. Compared with RO, NF can retain mineral elements in drinking water beneficial to human health, improve water yield, and has lower energy consumption [18]. It is a preferred water purification technology.

Codotte developed the first thin film composite (TFC) membrane with high performance by interfacial polymerization (IP), and it had become the foremost preparation method for NF membranes [19,20]. However, it is worth noting that most commercial TFC NF membranes are flat sheets. Compared with flat sheet membranes, hollow fiber membranes have such advantages as a higher packing density, larger specific surface area, lower energy consumption, higher rate of mass transfer, and easy to scale up [21–23]. Wei et al. [6,24] fabricated a NF hollow fiber membrane via IP with piperazine (PIP) and trimethyl chloride (TMC) as reactive monomer and Na_3PO_4 as the acid acceptor on the inner surface of a polysulfone (PSf)/polyethersulfone (PES) supporting membrane. The NF membrane had a rejection of 96.5% for $MgSO_4$ and a pure water flux (PWF) of 47.5 L/m^2/h at 4 bar. Li et al. [25] prepared a positively charged polyamide composite NF hollow membrane by IP of 1,4-Bis(3-aminopropyl) piperazine (DAPP) and TMC on the surface of a polyacrylonitrile (PAN) UF hollow fiber membrane. The rejection of $MgCl_2$ at a concentration of 1,000 mg/L was 73.4%, and the permeate flux was 6.5 L/m^2/h under 3 bar. Zhou et al. [26] fabricated a TFC NF hollow fiber membrane via IP with mixed PIP and 2,2′-bis (1-hydroxyl-1-trifluoromethyl-2,2,2-triflutoethyl)-4,4′-methylenedianiline (BHTTM) as water phase and TMC as the organic phase. The PWF of the NF membrane was 31.2 L/m^2/h and the rejection of Na_2SO_4 was 99.70% at 6 bar.

To our knowledge, although the current commercial NF membranes can retain monovalent salts in water to a large extent, the removal of polyvalent salts such as sodium sulfate, magnesium sulfate are still very high, usually more than 96% [6,24], and the removal of calcium chloride and magnesium chloride are also about 70% [25,26]. Many NF membranes are used to remove almost all the bivalent salts in water in other researches. This is contrary to the original intention to retain as much beneficial inorganic salts in drinking water as possible. An ideal NF membrane should have the characteristics of large water flux, high rejection rate to harmful substances, and low rejection to inorganic salts. Specifically, the larger the pore size of the NF membrane and/or the thinner the active layer, the greater the water flux and the lower the rejection of inorganic salts [27].

Obviously, the decreased rejection to inorganic salts of NF membranes will also cause the increased risk of heavy metal ions and small molecular chemicals such as pesticides and herbicides penetrating the membrane in the water, if any [18]. Moreover, in the process of municipal tap water pipeline transportation, due to the aging of pipeline valves, there are inevitably micro-pollution of tap water with heavy metals. If excessive heavy metals enter the human body through tap water, which accumulate in the human body for a long time, human health will be affected. Therefore, improved NF membranes for municipal tap water is needed, which not only produce mineral water for drinking, but also deal with the problem of heavy metal micro-pollution in tap water.

In order to achieve the above objective, the "trade-off" relationship between rejection and flux of the membrane can be used to adjust NF membrane performance, that is, the membrane rejection may be reduced appropriately to improve the membrane flux (and to reduce the operating pressure) [28]. In this study, a high flux, low rejection NF membrane hollow fiber was prepared by IP through adjusting the mass fractions and reaction time of PIP in water phase and organic phase TMC on the suface of PSf UF hollow fiber membrane. *N*-hexane was used as the organic solvent and camphorsulfonic acid triethylamine salt (CSA–TEA) was used as a surfactant in the aqueous phase. It is expected to reduce the rejection of beneficial minerals in tap water, such as Ca^{2+} and Mg^{2+} ions, and further reduce the operating pressure and improve the water recovery rate. Then, attenuated total reflectance–fourier transform infrared spectroscopy (ATR–FTIR), x-ray photoelectron spectroscopy (XPS), atomic force microscope (AFM), field emission scanning electron microscopy (FE-SEM), zeta potential test, and rejection test of five inorganic salts were characterized by various methods described in detail below. In addition, because a reduction in the NF membrane rejection may cause heavy metal micro-pollution in tap water, several heavy metals that are relatively less harmful to the human body were used as simulated metal ions. While Fe^{3+} and Cu^{2+} are not particularly harmful, they can affect the color, turbidity, and even odor of water at low concentrations. Too much intake Fe^{3+} and Cu^{2+} can also be bad for liver [29,30]. Pb^{2+} can cause damage to the kidney and central nervous systems, liver and reproductive systems, basic cellular processes, and brain functions [1,31]. Therefore, Fe^{3+}, Cu^{2+}, Pb^{2+} were selected as simulated heavy metal ions, and their rejection tests under different conditions were conducted to determine whether the water could meet the "SDWQ (GB5749-2006)," so as to evaluate the risk of the membrane in the source of heavy metal micro-pollution.

2. Experimental

2.1. Materials and reagents

PSf (Ude P-3500) was obtained from Solvay, USA. N,N-dimethyl acetamide (DMAc, AR, Kermel Chemical Reagent Co., Ltd., Tianjin China) was used as solvent for casting solution. The MWCO of PSf membrane was tested with polyethylene glycols (PEG) with various molecular weights (PEG2000, 4000, 6000, 8000, 10000, and 20000, >99.5%, Kermel Chemical Reagent Co., Ltd., Tianjin China). PIP (99%, Kermel Chemical Reagent Co., Ltd., Tianjin China) and camphor sulfonate (CAS, >98%, Kermel Chemical Reagent Co., Ltd., Tianjin China)-triethylamine (TEA, AR, Tianjin Feng Chuan Chemical Reagent Technology Co., Ltd., China) composite catalyst dissolved in deionized water reacted with TMC (>99%, Aladdin Chemistry Company, China) dissolved in *n*-hexane (Kermel Chemical Reagent Co., Ltd., China) to form a polyamide functional layer.

Analytical grade inorganic salts such as sodium sulfate (Na_2SO_4), magnesium sulfate ($MgSO_4$), calcium chloride ($CaCl_2$), ferric sulfate ($Fe_2(SO_4)_3$), copper sulfate ($CuSO_4$), lead sulfate ($PbSO_4$) were purchased from Kermel Chemical Reagent Co., Ltd., Tianjin China. Hydrochloric acid (HCl, AR) (Kermel Chemical Reagent Co., Ltd., China) and sodium hydroxide solutions (NaOH, AR) (Kermel Chemical Reagent Co., Ltd., China) were used to regulate the pH of the feed solution. All chemicals were used directly.

2.2. Preparation of PSf UF hollow fiber membrane

The casting solution was poured into a spinning kettle and was allowed to defoam for 12 h before spinning. In the spinning process, nitrogen gas was injected into the spinning kettle at 0.2 MPa, and the casting solution was pumped at a steady flow rate of 20 mL/min through the spinneret using a metering pump. After passing through an air gap of 5 cm, the hollow fibe was immersed in a coagulation bath for phase separation, and then towed and collected using winding rollers. The coagulant bath temperature was 25°C, and the fiber take up speed was 6 m/min. Then the hollow fibers were stored in deionized water. The PSf hollow fibers had an inner diameter of 0.25 mm and external diameter of 0.4 mm. The PWF of PSf membrane was 110.0 L/m^2/h at 0.2 MPa. The MWCO of the PSf hollow fifiber membrane was measured via solute rejection experiments using PEG with various molecular weights as the neutral rejection probes [32]. According to the result of curve fitting, the MWCO of the PSf base membrane was 6,000.

2.3. Preparation of TFC NF membrane

PIP was dissolved in deionized water with a mass percent of 2%. Furthermore, CAS-TEA amine salt surfactants were added at a mass percent of 2% and 1%. The mass contents of PIP and TMC were determined as described in a previous study [33] and other literatures. After the salt was completely dissolved, the PSf hollow fiber support membrane was immersed in the aqueous phase at least 10 min to make sure an adsorption equilibrium between micropores on the PSf supporting membrane and the aqueous phase was achieved. Excess liquid on the membrane surface was removed the using filter paper and the hollow fibers was then immersed in the organic phase solution with 0.15 wt.% TMC in *n*-hexane for 15 s. Then, a polyamide functional layer was fabricated on the top surface of the PSf base hollow fiber membrane. Finally, PSf membrane was air-dried at room temperature, and stored in a 30% glycerin aqueous solution for the following characterization and testing.

2.4. Characterization of TFC NF hollow fiber membrane

ATR-FTIR (Nicolet iS50, America) was used to analyze the chemical bond and the functional groups on the surface of the membrane. FTIR spectra with wavelengths between 1,400 and 3,800 cm^{-1} were recorded. XPS (*K*-alpha, Thermofisher, America) was used to confirm the chemical compositions of the outside surface. The spectra in a binding energy range of 100–800 eV was recorded. The surface region topology and roughness of base membrane and composite membrane before and after IP were provided by an AFM (Multimode 3, Bruker Co., Germany). All membranes filaments were dried before testing. Before running these tests, all samples were kept dry and clean. FE-SEM (Hitachi, S-4800, Japan) was applied to observe the cross sections and surface morphology using a working voltage of 15 kV. The hollow fibers were immersed in liquid nitrogen and cracked before testing, followed by coating with gold.

The surface zeta potential of the fabricated TFC NF hollow fiber membrane was determined through streaming potential measurements at various pH values ranging from 3 to 10. The test was performed with a solid surface zeta potential analyser (Surpass-3, Anton Paar GmbH, Austria). 1 mmol/L potassium chloride (KCl) (Kermel Chemical Reagent Co., Ltd., China) electrolyte solution was used to fill a cylindrical sample chamber containing the membrane samples. The pH of the KCl electrolyte solution was adjusted by a 0.1 mol/L HCl and a 0.1 mol/L NaOH.

2.5. NF membrane performance

Each membrane module was comprised of about 15 membrane filaments, with an effective length of about 20 cm. The outer diameter of the membrane was about 0.4 mm, and the effective filtration area per component was about 0.38 cm^2. A cross-flow filtration unit was used to measure model solution flux. The membranes performance was evaluated using a device shown in Fig. 1. In all experiments, outside-in hollow fiber filtration mode was used. Before NF experiments, all NF hollow fiber membranes were prepressurized under 0.5 MPa for 0.5 h with DI water to make sure the membranes were in the steady state. Each experiment was carried out for an hour. For each step, samples of permeate and reject solutions were taken after a 60 min filtration run, which was found to be sufficient to reach constant flow and rejection. All experimental results were averaged over three trials.

The PWF (L/m^2/h) is one of the important indexes to characterize the permeability of membrane. PWF was calculated through following Eq. (1) [34,35]:

$$\mathrm{PWF} = \frac{Q}{A \cdot t} \tag{1}$$

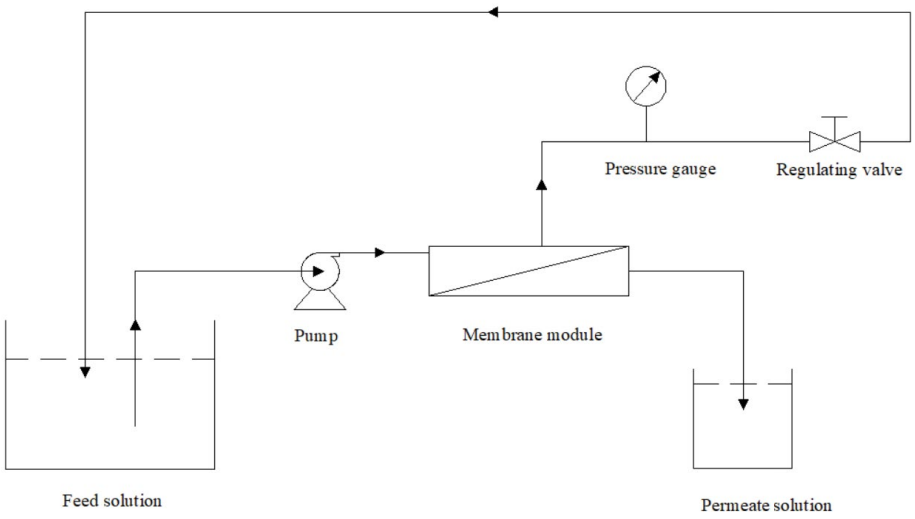

Fig. 1. Experimental set-up used in the experiments.

where Q is the volume of water permeated in a given period of time t. A is the effective filtration area of the hollow fiber membrane.

The permeability and rejection of Na_2SO_4, $MgSO_4$, $MgCl_2$, $CaCl_2$, and NaCl (1,000 mg/L) as feed solution were tested same as above. The rejection was calculated by the following Eq. (2) [34,35]:

$$R = \frac{C_1 - C_2}{C_1} \times 100\% \quad (2)$$

where R means the rejection rate, C_1 and C_2 are the concentration of feed and permeate solutions, respectively. The concentrations of the salt solutions were measured based on electric conductance.

2.6. Rejection behavior of NF membrane to heavy metals

In this study, three heavy metal ions Fe^{3+}, Cu^{2+}, and Pb^{2+} were selected as simulated ions of micro-pollution heavy metals in tap water. The rejections of the NF membrane to these heavy metal ions were studied under different conditions. Heavy metal ion concentrations were determined based on the "SDWQ (GB5749-2006)" in Table 1.

The effects of applied pressure (0.1–0.5 MPa), feed concentration (2–6 times the standard limit concentration of these ions), different inorganic salts (Na_2SO_4, $MgSO_4$, NaCl, $MgCl_2$), long-term stability (12 months) on the removal of Fe^{3+}, Cu^{2+}, and Pb^{2+} by the NF membrane were investigated. Rejections of heavy metal solutes can be calculated with Eq. (2). The concentrations of Fe^{3+}, Cu^{2+}, and Pb^{2+} were determined by inductively coupled plasma-mass spectrometry (7700E, Agilent, USA).

Table 1
Standards for Drinking Water Quality (SDWQ) (GB5749-2006) (partial)

Index	Criterion
Cu^{2+} (mg/L)	1.0
Pb^{2+} (mg/L)	0.01
Fe^{3+} (mg/L)	0.3
Chloride (mg/L)	250
Sulphate (mg/L)	250

3. Results and discussion

3.1. Structure characterization of TFC NF membranes

Fig. 2 is the ATR–FTIR survey spectra of the PSf UF hollow fiber support membrane (a) and the composite membrane after IP (b). The vibration bonds of polyamide functional groups (tertiary amide) appeared at 1,650 cm^{-1} (C=O stretching peaks) and 1,450 cm^{-1} (stretching vibration band of C–N) [36,37]. At the same time, in the region of 3,200–3,600 cm^{-1} a wide stretch hydroxyl group (O–H) characteristic peak appeared, indicating the carboxylic (–COOH) functional groups resulted from partial hydrolysis of residual acyl chloride groups of TMC occurred on the top layer of composite NF membrane [38,39].

Fig. 3 shows the chemical composition of the PSf UF and the TFC NF hollow fiber membrane surface assessed by XPS analysis. It was obvious that there were two same major emission peaks at 291.9 and 532.5 eV before (Fig. 3a) and after (Fig. 3b) IP, which were attributed to C_{1s} and O_{1s}, respectively. Additionally, two small peaks at 169.1 and 233 eV belonging to S_{2p} and S_{2s} originating from the sulfone groups were found, and the peak intensities of PSf UF was stronger than those observed for the TFC NF membrane, because the surface functional layer contained no elemental sulfur. It can be observed that a new emission peak appeared at 400 eV (Fig. 3b) compared with PSf UF membrane (Fig. 3a), which was attributed to N_{1s} from the amide group after IP. The atomic contents of C, N, O, and S elements were determined by XPS spectra, and the results are shown in Table 2. Compared with PSf UF hollow fiber substrate, nitrogen and oxygen contents of TFC NF membrane increased from 0%

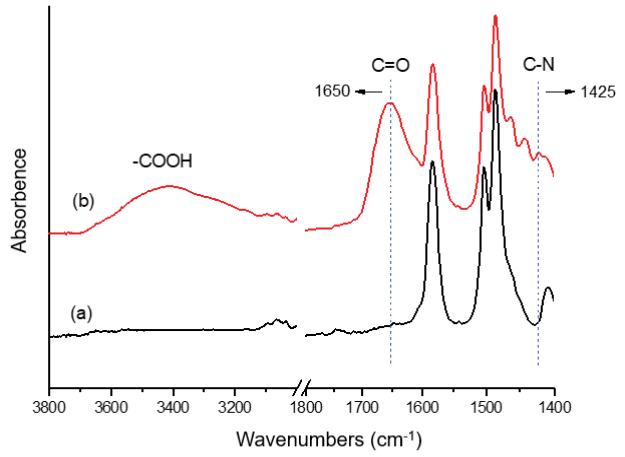

Fig. 2. ATR–FTIR spectra of (a) the PSf UF hollow fiber support membrane and (b) polyamide composite NF membrane after IP.

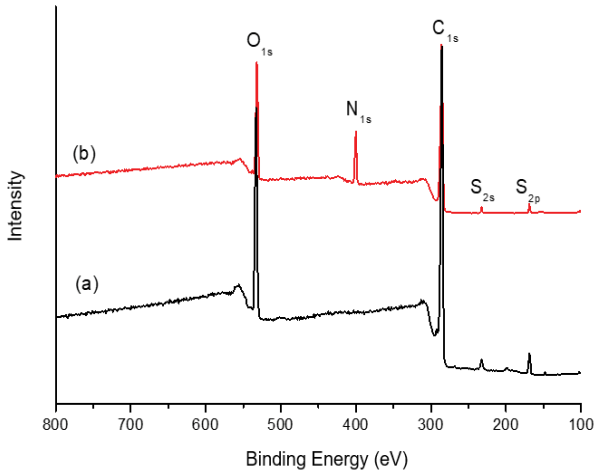

Fig. 3. XPS spectra of (a) the PSf UF hollow fiber supporting membrane and (b) polyamide composite NF membrane.

Table 2
Elements content of the membrane surface from XPS spectra

Membrane	PSf-UF	TFC-NF
C (%)	77.2	64.0
N (%)	–	13.0
O (%)	19.2	22.6
S (%)	3.6	0.4
O/C (×10^{-2})	24.9	35.3
N/C (×10^{-2})	–	20.3

and 19.2% to 13.0% and 22.6%, respectively. In contrast, the C and S contents decreased from 77.2% and 3.6% to 64.0% and 0.4%, respectively. The O/C ratio of TFC NF membrane was higher than that with PSf UF substrate because of the existence of acidamide group (–NHCO–) fabricated through IP.

Fig. 4 is the surface microstructures and cross-sections of PSf UF membrane and the TFC NF membrane observed using FE-SEM. The top surface of PSf (Fig. 4a) was smooth, whereas the surface of TFC NF membrane was rough with loosely distributed small nodules (Fig. 4a) caused by aggregated particle of a typical polyamide layer formed with IP [40]. These results are consistent with the conclusion of the AFM tests shown in Fig. 5b. It was remarkable that the hollow fiber membrane did not have traditional finger-like pores but sponge-like pores (Fig. 4b), and these sponge-like micropores became gradually smaller from the inside to the outside. That is, the membrane structure was gradually densified from the inside to the outside. The outer compact microporous structure was conducive to support a thinner polyamide desalination functional layer, thus reducing membrane resistance and achieving higher membrane flux. As shown in Fig. 4c and Fig. 4c′, the dense active skin layer with a thickness of 100 nm around firmly was attached to the support hollow fiber membrane. Compared to the skin thickness of 200–300 nm for commercial membranes [41], the NF membrane had a much thinner dense surface layer.

Fig. 5 is the AFM images and the roughness of the hollow fiber membrane before and after IP. Before IP, the average roughness (R_a) and RMS roughness (R_{rms}) of hollow fiber base membrane were 54.0 and 67.4 nm (Fig. 5a), respectively. After IP, the R_a and R_{rms} increased to 104 and 123 nm (Fig. 5b). After IP, a relatively thick and rough ridge-and-valley like polyamide layer was formed on the PSf substrate surface [42]. Fig. 4c′ also confirmed this observation. Fig. 5a shows the microstructure oriented along the fiber axis. This was due to the hollow fiber membrane in the forming process along the fiber axial tension. Overall, all the results characterized by ATR-FTIR, XPS, AFM, and SEM confirmed that the polyamide functional layer was successfully coated on the surface of the PSf UF base membrane.

3.2. Zeta potential of the TFC NF hollow fiber membrane surface

The surface charge property of the composite hollow fiber membranes has a significant influence on the rejection performance. The surface charge was determined in terms of zeta potential. Fig. 6. shows the zeta potential of the TFC NF hollow fiber membrane surface at different pH values ranging from 3 to 10. It can be found that the resultant membrane had an isoelectric point at pH 4.5. It indicated that the composite hollow fiber membrane was positively charged at the pH less than 4.5, which was attributable to the protonation of the amine functional groups on the top surface on the membrane [43]. In contrast, the membrane was negatively charged in the condition that pH values were above 4.5 in virtue of ionization of carboxyl (–COOH) groups and the deprotonation of amine functional groups.

3.3. Desalting performance of TFC NF membrane

Fig. 7 shows the performance of the PSf and TFC NF hollow fiber membranes under different pressuress in cross flow filtration. The pure water fluxes were positively correlated to the operating pressure and a linear relationship was observed. The pure water fluxes of PSf and TFC NF

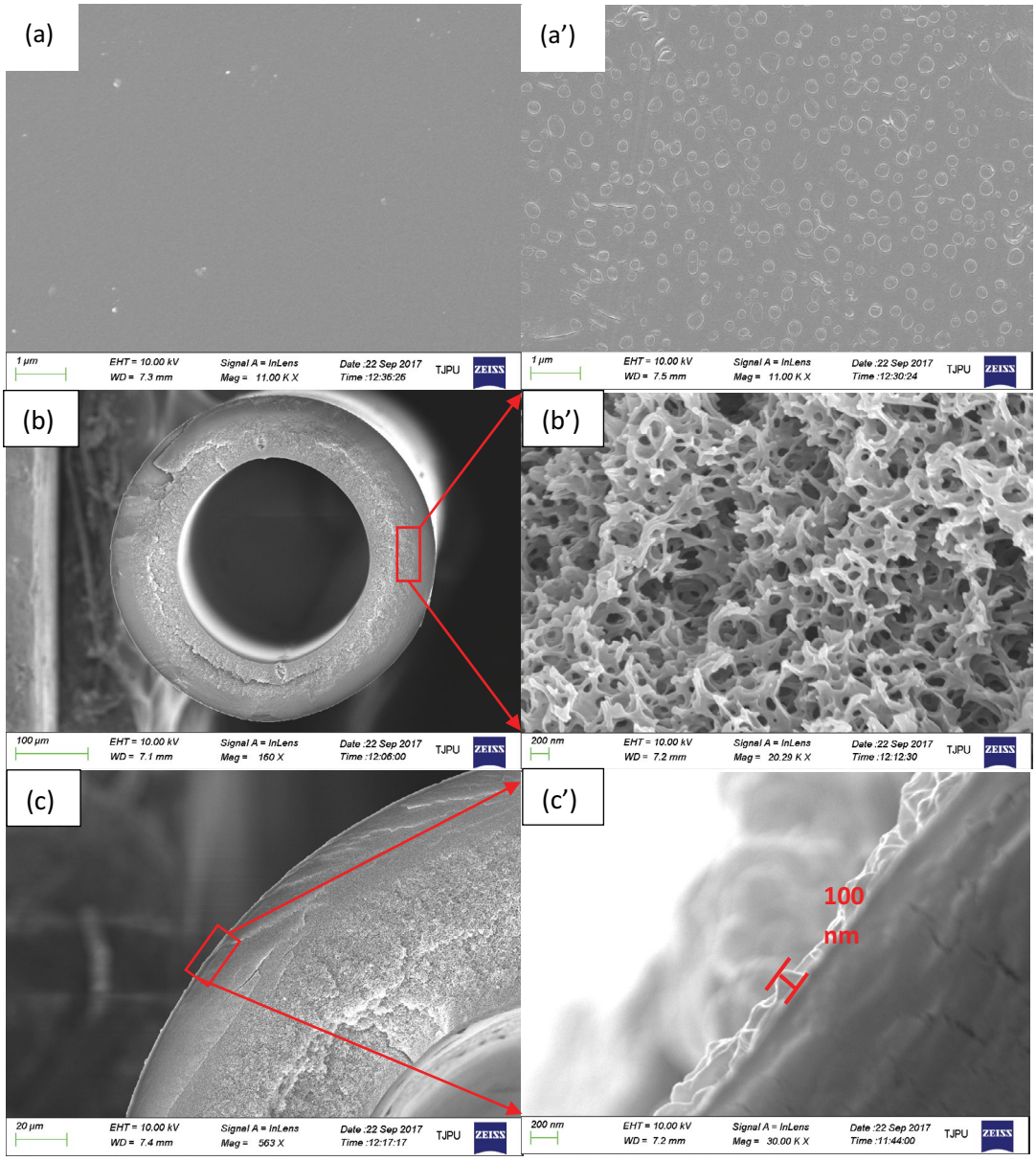

Fig. 4. FE-SEM images of the PSf UF supporting membrane and the TFC NF membrane (a) top surface of PSf UF hollow fiber membrane, (a') top surface of TFC NF hollow fiber membrane, (b, b', c, and c') cross-section of TFC NF hollow fiber membrane.

membrane can reach 110.0 and 41.3 L/m^2/h, respectively, at a pressure of 0.2 MPa.

Fig. 8 shows the separation performance of TFC NF membrane on the rejections and permeate fluxes of different inorganic salts $MgSO_4$, Na_2SO_4, $MgCl_2$, $CaCl_2$, and NaCl. The five inorganic salts had a concentration of 1,000 mg/L. The salt rejections were on the order of Na_2SO_4 > $MgSO_4$ > $MgCl_2$ > $CaCl_2$ > NaCl, which was consistent with other reports [26,44,45], and the order of permeate fluxes was reversed. The separation performance of TFC NF membrane results from size exclusion and electrical interactions between the inorganic salt ions and the charged membrane surface [46]. During the process of IP, parts of chloride groups on TMC hydrolyzed to yield carboxyl groups (–COOH). Additionally, the formation of the polyamide layer was accompanied by the presence of ammonium ions ($–NH_4^+$) partially [47,48]. The existence of these two functional groups endows the surface of the membrane with an electrical charge. The rejections of Na_2SO_4 and Mg_2SO_4 were higher than $MgCl_2$, $CaCl_2$, and NaCl, because the surface of the NF membranes are usually negatively charged [25,49], and the adsorption of divalent salt ions is higher than monovalent salt ions, and the repulsion of divalent anion (SO_4^{2-}) is stronger than monovalent anion (Cl^-). From the aspect of steric hindrance effect, the hydrated radius of SO_4^{2-} (3.79×10^{-10} m) is larger than that of Cl^- (3.32×10^{-10} m) [24], which makes sulfate ions to pass through the NF membrane more difficultly than chloride ions. The hydrated radius of Mg^{2+} and Ca^{2+} are 4.28 and 3.3 angstrom [50], respectively, and the steric-hindrance effect played a leading role in the

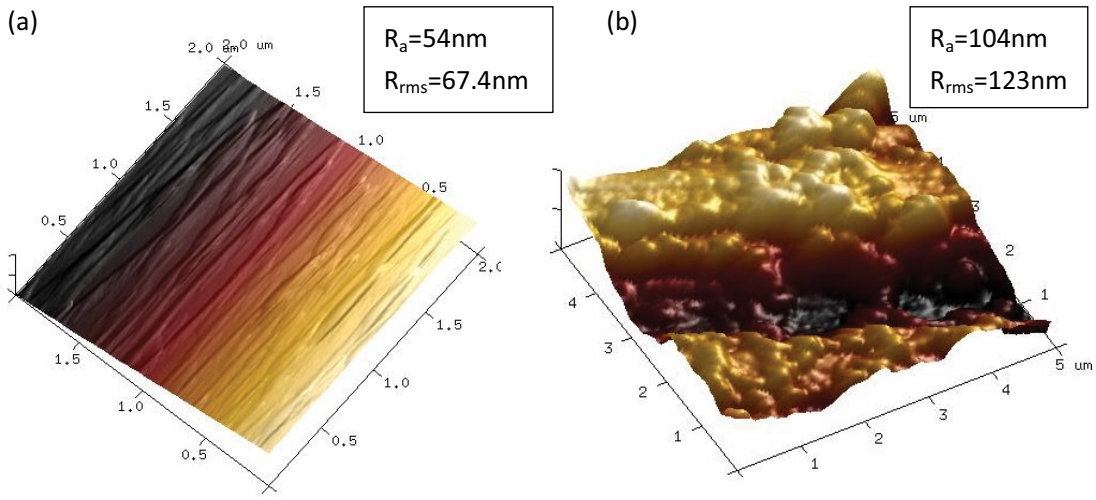

Fig. 5. AFM images and roughness before (a) and after (b) IP.

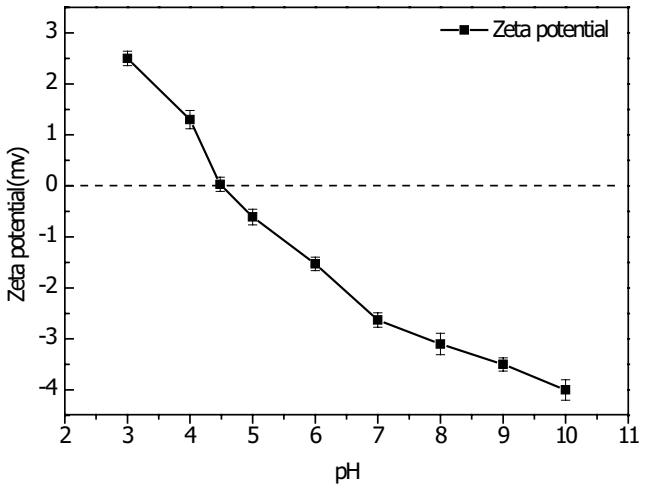

Fig. 6. Zeta potential of the composite TFC NF hollow fiber membrane at diverse pH values.

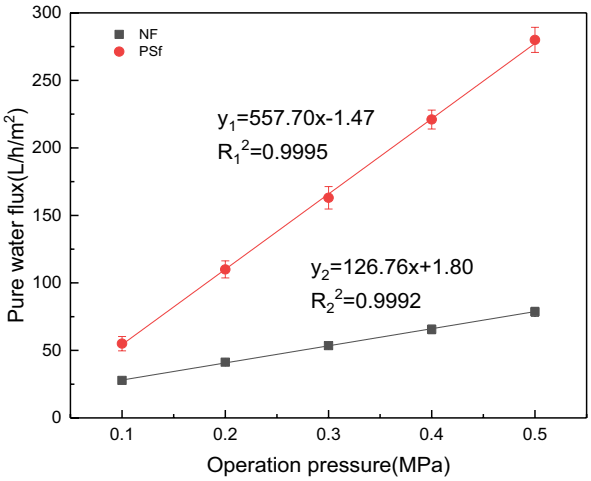

Fig. 7. Pure water flux of PSf and TFC NF membrane under different operation pressures.

rejections of $CaCl_2$ and $MgCl_2$. Smaller hydrated radius ions (Ca^{2+}) are more likely to pass through the membrane, so the rejection of $CaCl_2$ was lower than that of $MgCl_2$.

3.4. Rejection behavior of NF membrane on heavy metals

3.4.1. Effects of applied pressure on heavy metal ions rejection

Fig. 9 shows the influences of pressure on the rejection of the TFC NF membrane to heavy metals. The initial concentrations of Fe^{3+}, Cu^{2+}, and Pb^{2+} were 0.6, 2.0, and 0.02 mg/L, respectively. From Fig. 9, the rejections of heavy metals increased with an increase in the pressure. The rejection of Fe^{3+} increased from 90.7% to 95%, and the rejections of Cu^{2+} and Pb^{2+} increased from 89.5% and 82% to 93.5% and 88.4%, respectively. The reason for this trend was that as pressure increased, water permeation became faster. However, the increase of pressure would not significantly affect the solute diffusion rate because that solute diffusion rate was mainly controlled by the solute concentration [51]. As a result, the membrane rejection increased as the pressure increased. Similar results can be found in other studies [1,52–54]. The results showed that the rejection of Fe^{3+} was the highest (above 90%), followed by Cu^{2+}, and Pb^{2+} was the lowest. The reason for the order was because the hydrated ionic radius of Fe^{3+} is 4.57 angstrom, larger than Cu^{2+} (4.19 Å) and Pb^{2+} (4.01 Å), so the Fe^{3+} was more difficult to pass through the membrane [55]. It was worth nothing that in the condition of neutral aqueous solution, high content of hydroxyl ions (OH^-) led to the formation of Fe $(OH)_3$ and a metal hydroxide precipitate. In addition, the amount of iron ions existed in the form of the complexes $[Fe(H_2O)_6]^{3+}$, and the hydrated ion was bulky and difficult to pass through the membrane [26]. Therefore, the rejection of Fe^{3+} in neutral aqueous solution was much higher than that of Cu^{2+} and Pb^{2+}.

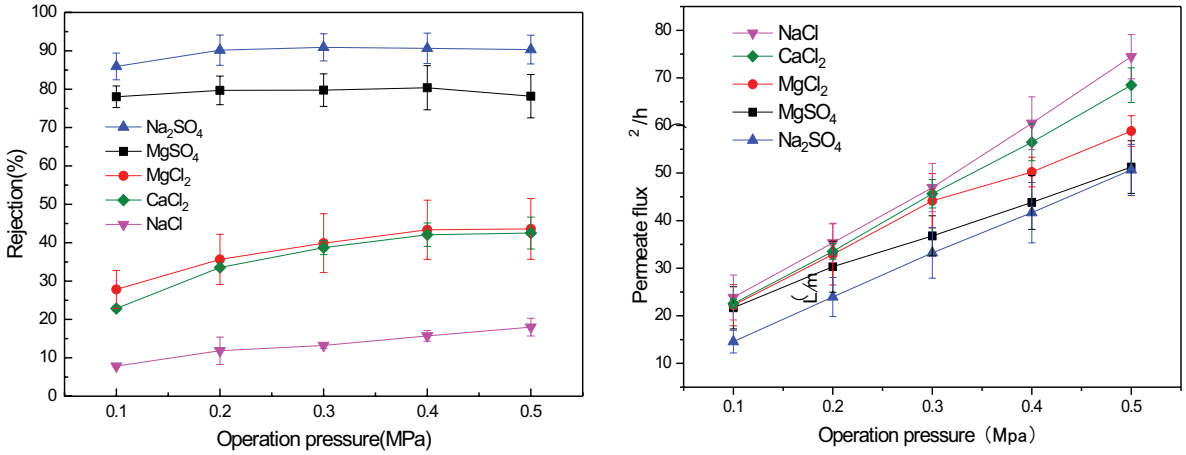

Fig. 8. Rejection and permeate flux of different salt solution under different operation pressures.

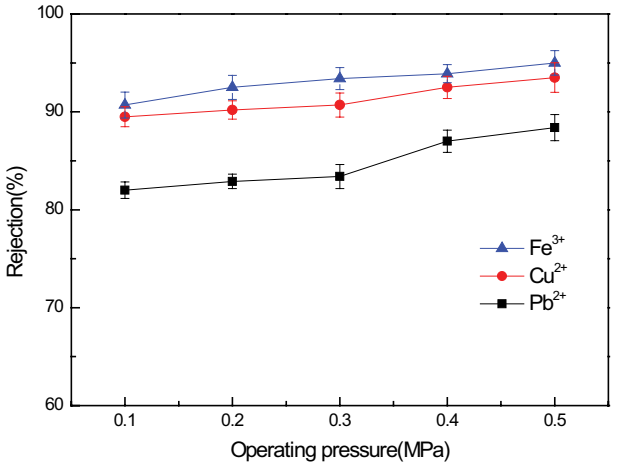

Fig. 9. Influence of pressure on the rejection of different heavy metals.

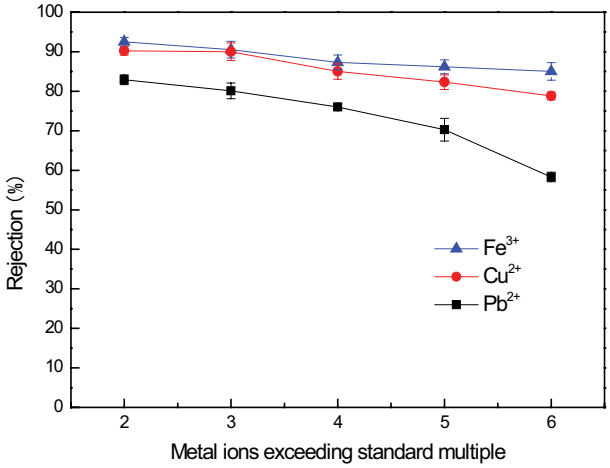

Fig. 10. Effects of initial concentration on the rejection of heavy metal ions.

3.4.2. Effect of metal concentration on composite NF membrane rejection

Heavy metal ions in municipal tap water are usually at very low concentrations. An important target of this study was to investigate the removal of heavy metal ions from the solutions with very low metal concentrations. Therefore, a series of tests were carried out to determine the concentration range of the heavy metals by the NF membrane under the conditions of constant metal ions concentrations (2–6 times the national standard) at 0.2 MPa.

Fig. 10 shows the effects of feed concentration on heavy metal ion rejections of the TFC NF membrane at 0.2 MPa. It was clear that high rejection rates (>85%) were observed for Fe^{3+} in the whole concentration range. Furthermore, for Cu^{2+}, the rejections were greater than 80%, which indicated that the metal concentrations in permeate were always below the limit concentration of SDWQ. As for Pb^{2+}, the rejection rates were all greater than 76% in the concentrations range from 0.01 to 0.03 mg/L. It was indicated that in this concentration range, the membrane can effectively intercept the lead ions. Meanwhile, it was observed that the rejection decreased as the concentration increased, which can be explained from the increased smotic pressure at higher feed concentrations. The osmotic effect resulted in less solvent passing through the membrane.

3.4.3. Effect of coexisting salt ion concentration on rejection of heavy metal ions

The municipal tap water often contains a variety of salt ions. Here, four common inorganic salts (Na_2SO_4, $MgSO_4$, NaCl, and $MgCl_2$) in tap water were selected as coexisting ions of heavy metal solutions of Fe^{3+}, Cu^{2+}, and Pb^{2+}. The initial concentrations of Fe^{3+}, Cu^{2+}, and Pb^{2+} were 0.6, 2.0, and 0.02 mg/L, respectively. All the experiments were conducted under 0.2 MPa, at different concentrations of inorganic salts. The performance of the NF membrane to retain heavy metal ions was investigated.

Fig. 11 shows the effects of the four inorganic salt on the removal of heavy metal ions. The rejection rates of the membrane for Fe^{3+} and Cu^{2+} decreased with the addition of

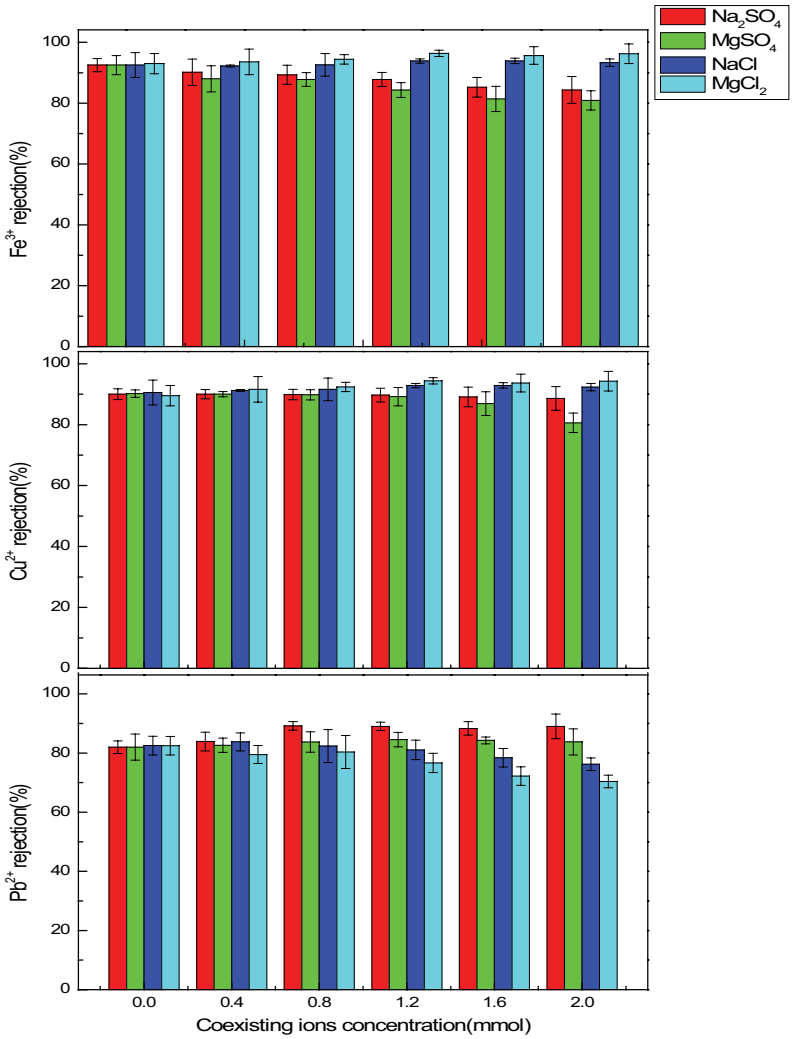

Fig. 11. Effect of coexisting salt (Na_2SO_4, $MgSO_4$, NaCl, and $MgCl_2$) concentration on rejection of Fe^{3+}, Cu^{2+}, and Pb^{2+}.

sulfate, but increased with the addition of chloride, while the rejection of Pb^{2+} was just the opposite. Moreover, compared with Mg^{2+} salt and Na^{+} salt at the same concentration, the effect of divalent magnesium salt was more obvious. This was mainly due to the charge effect on the membrane surface. The addition of cations reduced the negative charge on the NF membrane surface and weakened the Donnan effect between heavy metal ions and the NF membrane [56]. The divalent ion Mg^{2+} weakened the negative charge on the surface of the NF membrane to a greater extent. In addition, the complex ions competition in the mixed system also led to slightly different results. Overall, the rejection rates of all heavy metal ions were still above 70%, meeting the national drinking water requirements.

3.4.4. Long-term stability of the NF membrane for rejection of heavy metal ions

In order to evaluate the stability and the reusability of the NF membrane, a 12-month dynamic filtration experiment was conducted on the membrane in the laboratory. The initial concentrations of Fe^{3+}, Cu^{2+}, and Pb^{2+} were 0.6, 2.0, and 0.02 mg/L, respectively. All the experimental operations were conducted at 0.2 MPa. The stability and repeatability were investigated by observing the permeate fluxes and rejections of the heavy metal. As shown in Fig. 12, the permeate flux and the heavy metal rejection of the did not change significantly over the 12-month period.

3.5. Comparison of the prepared membrane with other reported membranes

Table 3 shows the desalination properties of membranes prepared using different concentrations of PIP in the aqueous phase and TMC in the organic phase used in IP reported in the literature. In this study, a TFC NF membrane was obtained by spinning a denser PSf (PEG6000) membrane support and a shorter IP time. Compared with previous studies [38,39,57,58], the prepared PSf membrane had smaller MWCO, denser support layer and shorter surface IP time. This was to ensure that the substrate membrane had a thinner surface functional layer so as to reduce the water transmission resistance without scarifying the mechanical strength. The newly prepared NF

Table 3
Comparison of mean mass fractions of PIP and TMC, salt permeation flux, $MgSO_4$ rejection and operating pressure (ΔP) of NF membrane with the same IP with other literature data

Psf (MWCO)	PIP mass fraction and reaction time	TMC mass fraction and reaction time	Salt permeation flux (L/m²/h)	$MgSO_4$ rejection (%)	ΔP (MPa)	Reference
Hollow fiber membrane (6,000)	2 wt.%,10 min	0.15 wt.%, 15 s	30.07	79.68	0.2	This study
			43.97	80.38	0.4	
Sheet membrane (20,000)	2 wt.%,15 min	0.05 wt.%, 30 s	~25	~89	0.7	[38]
Sheet membrane (520,000)	2 wt.%,10 min	0.1 wt.%, 30 s	~23.5	~95	0.7	[57]
Hollow fiber membrane (20,000)	0.2 wt.%, 30 min	0.12 wt.%, 2 min	32.6	98.13	0.7	[58]
Sheet membrane (50,000)	1 wt.%,3 min	0.15 wt.%, 15 s	~22	(Na_2SO_4) 97	0.6	[39]

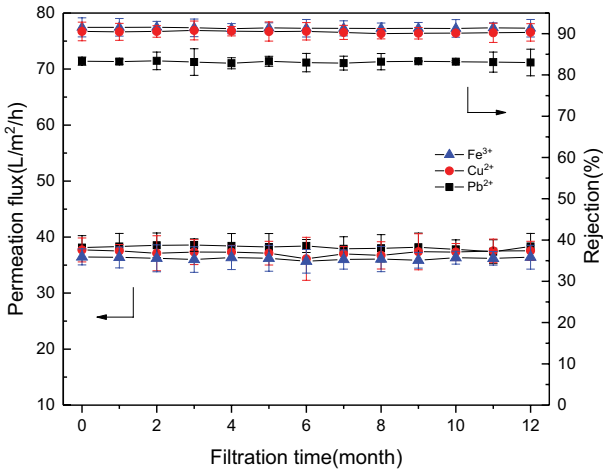

Fig. 12. Long-term stability test of the NF membrane on rejection of heavy metal ions.

membrane obviously had a higher permeate flux at a lower operating pressure. The rejection of $MgSO_4$ was reduced to 79.68% and the flux increased to 30.07 L/m²/h, which was more in line with the requirements of tap water in practical applications [3]. It not only retained some of the minerals needed by the human body, but also increased the water production rate.

4. Conclusions

A novel TFC NF membrane was prepared by IP on the surface of a PSf substrate with controlled PIP and TMC concentrations. A thinner polyamide selective layer (<100 nm) than commercial NF membranes was successfully coated on the PSf UF membrane surface. The NF membrane needed a lower operating pressure, produced a higher water flux with lower desalination rates, which helped better retain the beneficial substances and prevent excessive purification of tap water. Based on the evaluation of heavy metal micro-pollution in tap water, when the concentration of heavy metal ions increased to three times of the "SDWQ (GB5749-2006)," the rejections on Fe^{3+}, Cu^{2+}, and Pb^{2+} of the NF membranes were all above 76%, which was in line with the drinking water sanitation standard. In addition, the NF membrane showed long-term stability and reusability. In conclusion, the prepared NF membrane can ensure the production of healthy drinking water and avoid the risk of heavy metal micro-pollution in the water.

Acknowledgment

The authors gratefully acknowledge the financial support from Major Science and Technology Program for Water Pollution Control and Treatment (2017ZX07107-001), the National Natural Science Foundation of China (Grant No. 51678410), and the National High Technology Research and Development Program of China (Grant No. 2012AA03A602). Special thanks would be given to Professor Xianshe Feng for his advice and modifications to the manuscript.

References

[1] A. Maher, M. Sadeghi, A. Moheb, Heavy metal elimination from drinking water using nanofiltration membrane technology and process optimization using response surface methodology, Desalination, 352 (2014) 166–173.
[2] Y.-l. Liu, X.-m. Wang, H.-w. Yang, Y.F. Xie, X. Huang, Preparation of nanofiltration membranes for high rejection of organic micropollutants and low rejection of divalent cations, J. Membr. Sci., 572 (2019) 152–160.
[3] K. Sutherland, Drinking & other pure water production: filtration and sedimentation in clean water production, Filtr. Sep., 51 (2014) 24–27.
[4] N. Hilal, H. Al-Zoubi, N.A. Darwish, A.W. Mohamma, M. Abu Arabi, A comprehensive review of nanofiltration membranes: treatment, pretreatment, modelling, and atomic force microscopy, Desalination, 170 (2004) 281–308.
[5] Y. Lv, H.-C. Yang, H.-Q. Liang, L.-S. Wan, Z.-K. Xu, Nanofiltration membranes via co-deposition of polydopamine/polyethylenimine followed by cross-linking, J. Membr. Sci., 476 (2015) 50–58.
[6] X. Wei, X. Kong, S. Wang, H. Xiang, J. Wang, J. Chen, Removal of heavy metals from electroplating wastewater by thin-film composite nanofiltration hollow-fiber membranes, Ind. Eng. Chem. Res., 52 (2013) 17583–17590.
[7] S. Wang, Y. Zhou, C. Gao, Novel high boron removal polyamide reverse osmosis membranes, J. Membr. Sci., 554 (2018) 244–252.
[8] A. Zhang, R. Ma, Y. Xie, B. Xu, S. Xia, N. Gao, Preparation polyamide nanofiltration membrane by interfacial polymerization, Desal. Water. Treat., 37 (2012) 238–243.
[9] P. Mou, S.D. Jons, Chemistry and fabrication of polymeric nanofiltration membranes: a review, Polymer, 103 (2016) 417–456.
[10] S. Benedetti, E.S. Prudêncio, J.M.G. Mandarino, K. Rezzadori, J.C.C. Petrus, Concentration of soybean isoflavones by

nanofiltration and the effects of thermal treatments on the concentrate, Food. Res. Int.,50 (2013) 625–632.
[11] N. Ghaemi, P. Daraei, F.S. Akhlaghi, Polyethersulfone nanofiltration membrane embedded by chitosan nanoparticles: fabrication, characterization and performance in nitrate removal from water, Carbohydr. Polym., 191 (2018) 142–151.
[12] P.S. Zhong, N. Widjojo, T.-S. Chung, M. Weber, C. Maletzko, Positively charged nanofiltration (NF) membranes via UV grafting on sulfonated polyphenylenesulfone (sPPSU) for effective removal of textile dyes from wastewater, J. Membr. Sci., 417 (2012) 52–60.
[13] A.J. Hargreaves, P. Vale, J. Whelan, L. Alibardi, C. Constantino, G. Dotro, E. Cartmell, P. Campo, Impacts of coagulation-flocculation treatment on the size distribution and bio-availability of trace metals (Cu, Pb, Ni, Zn) in municipal wastewater, Water Res., 128 (2018) 120–128.
[14] A.Y. Zahrim, C. Tizaoui, N. Hilal, Coagulation with polymers for nanofiltration pre-treatment of highly concentrated dyes: a review, Desalination, 266 (2011) 1–16.
[15] F. Salehi, Current and future applications for nanofiltration technology in the food processing, Food Bioprod. Process., 92 (2014) 161–177.
[16] J. Zhu, S. Yuan, A. Uliana, J. Hou, J. Li, X. Li, M. Tian, Y. Chen, A. Volodin, B.V. der Bruggen, High-flux thin film composite membranes for nanofiltration mediated by a rapid co-deposition of polydopamine/piperazine, J. Membr. Sci., 554 (2018) 97–108.
[17] A. Cihanoğlu, S. Alsoy Altinkaya, A facile approach for preparation of positively charged nanofiltration membranes by in-situ crosslinking between polyamide-imide and poly-ethylenimine, Sep. Purif. Technol., 207 (2018) 353–362.
[18] J.M. Gohil, P. Ray, A review on semi-aromatic polyamide TFC membranes prepared by interfacial polymerization: potential for water treatment and desalination, Sep. Purif. Technol., 181 (2017) 159–182.
[19] M. Fathizadeh, A. Aroujalian, A. Raisi, Effect of lag time in interfacial polymerization on polyamide composite membrane with different hydrophilic sub layers, Desalination, 284 (2012) 32–41.
[20] H. Karimi, A. Rahimpour, M.R. Shirzad Kebria, Pesticides removal from water using modified piperazine-based nanofiltration (NF) membranes, Desal. Water. Treat., 57 (2016) 24844–24854.
[21] C. Su, C. Lu, H. Cao, K. Tang, J. Chang, F. Duan, X. Ma, Y. Li, Fabrication and post-treatment of nanofibers-covered hollow fiber membranes for membrane distillation, J. Membr. Sci., 562 (2018) 38–46.
[22] A.C. Sun, W. Kosar, Y. Zhang, X. Feng, Vacuum membrane distillation for desalination of water using hollow fiber membranes, J. Membr. Sci., 455 (2014) 131–142.
[23] Y. Zhang, J. Wang, F. Gao, H. Tao, Y. Chen, H. Zhang, Impact of sodium hypochlorite (NaClO) on polysulfone (PSF) ultrafiltration membranes: the evolution of membrane performance and fouling behavior, Sep. Purif. Technol., 175 (2017) 238–247.
[24] X. Wei, X. Kong, C. Sun, J. Chen, Characterization and application of a thin-film composite nanofiltration hollow fiber membrane for dye desalination and concentration, Chem. Eng. J., 223 (2013) 172–182.
[25] X. Li, C. Zhang, S. Zhang, J. Li, B. He, Z. Cui, Preparation and characterization of positively charged polyamide composite nanofiltration hollow fiber membrane for lithium and magnesium separation, Desalination, 369 (2015) 26–36.
[26] B.-W. Zhou, H.-Z. Zhang, Z.-L. Xu, Y.-J. Tang, Interfacial polymerization on PES hollow fiber membranes using mixed diamines for nanofiltration removal of salts containing oxyanions and ferric ions, Desalination, 394 (2016) 176–184.
[27] G.M. Geise, H.B. Park, A.C. Sagle, B.D. Freeman, J.E. McGrath, Water permeability and water/salt selectivity tradeoff in polymers for desalination, J. Membr. Sci., 369 (2011) 130–138.
[28] O. Labban, C. Liu, T.H. Chong, J.H. Lienhard, Relating transport modeling to nanofiltration membrane fabrication: Navigating the permeability-selectivity trade-off in desalination pretreatment, J. Membr. Sci., 554 (2018) 26–38.
[29] A. Bera, J.S. Trivedi, S.B. Kumar, A.K.S. Chandel, S. Haldar, S.K. Jewrajka, Anti-organic fouling and anti-biofouling poly(piperazineamide) thin film nanocomposite membranes for low pressure removal of heavy metal ions, J. Hazard. Mater., 343 (2018) 86–97.
[30] R. Krachler, R.F. Krachler, G. Wallner, P. Steier, Y. El Abiead, H. Wiesinger, F. Jirsa, B.K. Keppler, Sphagnum-dominated bog systems are highly effective yet variable sources of bio-available iron to marine waters, Sci. Total Environ., 556 (2016) 53–62.
[31] W.-P. Zhu, S.-P. Sun, J. Gao, F.-J. Fu, T.-S. Chung, Dual-layer polybenzimidazole/polyethersulfone (PBI/PES) nanofiltration (NF) hollow fiber membranes for heavy metals removal from wastewater, J. Membr. Sci., 456 (2014) 117–127.
[32] T. Yang, C.F. Wan, J.Y. Xiong, T.-S. Chung, Pre-treatment of wastewater retentate to mitigate fouling on the pressure retarded osmosis (PRO) process, Sep. Purif. Technol., 215 (2019) 390–397.
[33] Y. Zhang, C. Xiao, E. Liu, Q. Du, X. Wang, H. Yu, Investigations on the structures and performances of a polypiperazine amide/polysulfone composite membrane, Desalination, 191 (2006) 291–295.
[34] B.A.M. Al-Rashdi, D.J. Johnson, N. Hilal, Removal of heavy metal ions by nanofiltration, Desalination, 315 (2013) 2–17.
[35] S. Ilyas, S.M. Abtahi, N. Akkilic, H.D.W. Roesink, W.M. de Vos, Weak polyelectrolyte multilayers as tunable separation layers for micro-pollutant removal by hollow fiber nanofiltration membranes, J. Membr. Sci., 537 (2017) 220–228.
[36] K. Hendrix, K. Vanherck, I.F.J. Vankelecom, Optimization of solvent resistant nanofiltration membranes prepared by the *in-situ* diamine crosslinking method, J. Membr. Sci., 421–422 (2012) 15–24.
[37] W. Li, C. Shi, A. Zhou, X. He, Y. Sun, J. Zhang, A positively charged composite nanofiltration membrane modified by EDTA for LiCl/$MgCl_2$ separation, Sep. Purif. Technol., 186 (2017) 233–242.
[38] H. Li, W. Shi, Y. Zhang, Q. Du, X. Qin, Y. Su, Improved performance of poly(piperazine amide) composite nanofiltration membranes by adding aluminum hydroxide nanospheres, Sep. Purif. Technol., 166 (2016) 240–251.
[39] S.-M. Xue, Z.-L. Xu, Y.-J. Tang, C.-H. Ji, Polypiperazine-amide nanofiltration membrane modified by different functionalized multiwalled carbon nanotubes (MWCNTs), ACS Appl. Mater. Interfaces, 8 (2016) 19135–19144.
[40] C.Y. Tang, Y.N. Kwon, J.O. Leckie, Effect of membrane chemistry and coating layer on physiochemical properties of thin film composite polyamide RO and NF membranes: I. FTIR and XPS characterization of polyamide and coating layer chemistry, Desalination, 242 (2009) 149–167.
[41] M. Fathizadeh, H.N. Tien, K. Khivantsev, Z. Song, F. Zhou, M. Yu, Polyamide/nitrogen-doped graphene oxide quantum dots (N-GOQD) thin film nanocomposite reverse osmosis membranes for high flux desalination, Desalination, 451 (2019) 125–132.
[42] W.-P. Zhu, J. Gao, S.-P. Sun, S. Zhang, T.-S. Chung, Poly(amidoamine) dendrimer (PAMAM) grafted on thin film composite (TFC) nanofiltration (NF) hollow fiber membranes for heavy metal removal, J. Membr. Sci., 487 (2015) 117–126.
[43] L. Setiawan, L. Shi, R. Wang, Dual layer composite nanofiltration hollow fiber membranes for low-pressure water softening, Polymer, 55 (2014) 1367–1374.
[44] W. Fang, L. Shi, R. Wang, Mixed polyamide-based composite nanofiltration hollow fiber membranes with improved low-pressure water softening capability, J. Membr. Sci., 468 (2014) 52–61.
[45] Q. Shi, L. Ni, Y. Zhang, X. Feng, Q. Chang, J. Meng, Poly(p-phenylene terephthamide) embedded in a polysulfone as the substrate for improving compaction resistance and adhesion of a thin film composite polyamide membrane, J. Mater. Chem. A, 5 (2017) 13610–13624.
[46] K. Linde, A.-S. Jönsson, Nanofiltration of salt solutions and landfill leachate, Desalination, 103 (1995) 223–232.

[47] S. Bouranene, P. Fievet, A. Szymczyk, M.E.-H. Samar, A. Vidonne, Influence of operating conditions on the rejection of cobalt and lead ions in aqueous solutions by a nanofiltration polyamide membrane, J. Membr. Sci., 325 (2008) 150–157.
[48] C.-V. Gherasim, J. Cuhorka, P. Mikulášek, Analysis of lead (II) retention from single salt and binary aqueous solutions by a polyamide nanofiltration membrane: experimental results and modelling, J. Membr. Sci., 436 (2013) 132–144.
[49] H. Wang, Q. Zhang, S. Zhang, Positively charged nanofiltration membrane formed by interfacial polymerization of 3,3′,5,5′-biphenyl tetraacyl chloride and piperazine on a poly (acrylonitrile) (PAN) support, J. Membr. Sci., 378 (2011) 243–249.
[50] G. Yang, I. Neretnieks, M. Holmboe, Atomistic simulations of cation hydration in sodium and calcium montmorillonite nanopores, J. Chem. Phys., 147 (2017) 084705.
[51] Z. Wang, G. Liu, Z. Fan, X. Yang, J. Wang, S. Wang, Experimental study on treatment of electroplating wastewater by nanofiltration, J. Membr. Sci., 305 (2007) 185–195.
[52] L.B. Chaudhari, Z.V. Murthy, Separation of Cd and Ni from multicomponent aqueous solutions by nanofiltration and characterization of membrane using IT model, J. Hazard. Mater., 180 (2010) 309–315.
[53] C.-V. Gherasim, P. Mikulášek, Influence of operating variables on the removal of heavy metal ions from aqueous solutions by nanofiltration, Desalination, 343 (2014) 67–74.
[54] Z. Murthy, L.B. Chaudhari, Separation of binary heavy metals from aqueous solutions by nanofiltration and characterization of the membrane using Spiegler–Kedem model, Chem. Eng. J., 150 (2009) 181–187.
[55] B. Tansel, J. Sager, T. Rector, J. Garland, R.F. Strayer, L. Levine, M. Roberts, M. Hummerick, J. Bauer, Significance of hydrated radius and hydration shells on ionic permeability during nanofiltration in dead end and cross flow modes, Sep. Purif. Technol., 51 (2006) 40–47.
[56] V. Freger, T. Arnot, J. Howell, Separation of concentrated organic/inorganic salt mixtures by nanofiltration, J. Membr. Sci., 178 (2000) 185–193.
[57] J. Jin, D. Liu, D. Zhang, Y. Yin, X. Zhao, Y. Zhang, Taurine as an additive for improving the fouling resistance of nanofiltration composite membranes, J. Appl. Polym. Sci., 132 (2015), doi: 10.1002/app.41620.
[58] H. Li, W. Wang, Y. Zhang, Preparation and characterization of high-selectivity hollow fiber composite nanofiltration membrane by two-way coating technique, J. Appl. Polym. Sci., 131 (2014), doi: 10.1002/app.41187.